Quantum Chemical Studies of Neutral and Ionized DyX, DyX_2, and DyX_3 Species (X = F, Cl, Br, I) and the Implications for the Mass Spectra of Gaseous DyX_3

Julia Saloni,[a,d] Szczepan Roszak,*[a] Klaus Hilpert,[b] Mirosław Miller,[c] and Jerzy Leszczynski[d]

Keywords: Halides / Lanthanides / Mass spectrometry / Quantum chemical calculations / Thermochemistry

The mass spectrum pattern of DyF_3(g) and the appearance potentials for identified ions were measured and compared with the respective data obtained previously for $DyCl_3$, $DyBr_3$, and DyI_3. The structural parameters, total energies, and vibrational frequencies of DyX_3, DyX_2, and DyX (X = F, Cl, Br, I) neutral and single ionized species were determined by quantum-chemical studies. The theoretical appearance potentials of different ions, calculated from energies of gaseous species, are in the good agreement with the experimental data. Fragmentation energies of the DyX_n^+ ion, where n = 1, 2, 3, were computed and compared with the mass spectra patterns of the respective vapour species. A theoretical electron population analysis indicates the involvement of the s and f valence electrons of Dy in the bond formation as well as in the ionization processes. The σ-back donation from halogen atoms to the dysprosium center partially compensates the electron density loss. The ionization strengthens the bonding in the DyX and DyX_2 molecules. The ionization of DyX_3 destroys the C_{3v} symmetrical structure due to the Jahn–Teller effect. Contrary to the other studied systems, the open shell character of DyX_3^+ arises not only from unpaired electrons of dysprosium but also from electron density on halogen atoms.

Introduction

Knudsen effusion mass spectrometric studies of metal halide vapors show evidence for the significant fragmentation of gaseous species due to the electron bombardment used for the ionization. The mechanism of the ionization and fragmentation processes leading to the formation of particular ions recorded in the mass spectra is poorly understood. The molecular structures and the bonding nature of the species taking part in such processes are not directly available experimentally, and supplementary theoretical data is usually scarce. The few combined experimental and theoretical studies (e.g. ref.[1]) that exist allow a discussion of the energetic considerations and a quantitative analysis of fragmentation data.[2,3] Unfortunately, experimental mass spectra for metal halides published in the literature depend, to some extent, on the construction of the ion source of the mass spectrometer and on the energy of the ionising electrons. In order to correlate the theoretical predictions of the mass spectrum patterns with experimental data, the "true" mass spectra, obtained by the integration of peak areas, not by recording their intensities, should be taken into account.[4] In spite of this, mass spectra of gaseous metal halides recorded by different authors show similar characteristic trends for the ion intensities. The highest thermodynamic stability is not necessarily the most important condition for that particular ion to be the most abundant in the mass spectrum. However, the structures, bonding, and the charge distribution of ions formed upon ionization/fragmentation processes should, to some extent, correlate with the mass spectrum. Moreover, as was shown previously,[1,3] the thermochemical stability of neutral species and ions can be used for the elucidation of the fragmentation behavior of gaseous species. The above considerations motivated the analysis of the structural and thermochemical properties of gaseous species obtained by experimental and theoretical approaches for metal halide systems presented in this work. The recent development of quantum chemical methods has resulted in the efficient sup-

[a] Institute of Physical and Theoretical Chemistry, Wroclaw University of Technology,
Wybrzeże Wyspiańskiego 27, 50-370 Wroclaw, Poland
Fax: (internat.) +48-71-320-3364
E-mail: roszak@mml.ch.pwr.wroc.pl
[b] Research Center Jülich, Institute for Materials and Processes in Energy Systems,
52425 Jülich, Germany
[c] Institute of Inorganic Chemistry and Metallurgy of Rare Elements, Wroclaw University of Technology,
Wybrzeże Wyspiańskiego 27, 50−370 Wroclaw, Poland
[d] Computational Center for Molecular Structure and Interactions, Jackson State University,
Jackson, MS 39217, USA

port of the theory of mass spectra in organic chemistry (e.g. ref.[5]). To the best of our knowledge, such studies for metal halide vapors are yet to be performed.

In the present study we report an experimental and quantum chemical analysis of neutral and ionic species detected upon studying the vaporization of DyX_3 by Knudsen effusion mass spectrometry. The vaporization of dysprosium halides has been investigated by different methods. Brunetti et al.[6] and Kapala et al.[7] have published a comparison of thermodynamic data reported in the literature. Recently, the vaporization thermodynamics of $DyCl_3$,[7,8] $DyBr_3$,[9] and DyI_3 [10] were investigated by means of Knudsen effusion mass spectrometry using different equipment and experimental conditions. The ion-molecule reactions in the $DyCl_3$ vapors were studied as well.[8] The mass spectrometric analysis of DyF_3 vapors performed in the present work complements our previous investigations.[7,9,10] The vapors of DyX_3 are predominantly monomeric, although mass spectrometric studies show evidence for dimeric,[7−10] trimeric,[8,10] or even tetrameric[8] species. In the past few years several quantum chemical studies have been carried out on gaseous lanthanide halides. The structures of monomeric[7,11−13] and dimeric[7,14] complexes of LnX_3 and other properties, including vibrational modes, have been presented. The results of the calculations were used for the interpretation of experimental infrared spectra of the gaseous phase[12] and for the estimation of the thermodynamic functions of gaseous species required for the third law treatment of equilibrium partial pressures.[7]

In the present work the theoretical structures and vibrational frequencies of DyX_3^+ molecular ions and their fragments (DyX_2^+, DyX^+) are reported. Their ionization potentials and appearance potentials were also calculated and compared with the values determined experimentally. The nature of the chemical bonding was studied applying Mulliken and natural bond orbital (NBO) electron population analysis. This information on structures, stabilities, and dissociation energies of gaseous ions is a significant step toward the better understanding of ionization and fragmentation processes in metal halide vapors and should thereby allow the prediction of their mass spectra.

Results

Mass Spectrometric Investigations

The mass spectrum of the DyF_3 vapors was recorded over a temperature range of 1208−1587 K. Table 1 shows the mass spectral data of gaseous DyF_3 interpolated for 1430 K. The data for gaseous DyX_3, where X = Cl, Br, I; obtained in previous studies are shown in Table 1 as well. The ionization of DyX_3 species by electron bombardment results, in addition to molecular ions, in the formation of DyX_n^+ fragments, where n = 0−2. Such fragmentation paths are generally characteristic for metal halide molecules (e.g. ref.[15]). The increasing fragmentation of gaseous DyX_3 on going from iodide to fluoride can easily be seen from the data in Table 1, despite the fact that they obtained with different spectrometers, at different temperatures, and with different energies of ionizing electrons. The same regularity can be seen for other metal halides.[15]

Table 1. Experimental mass spectra of the gaseous DyX_3 species

DyX_3	E_{el} (eV)	T (K)	DyX_3^+	DyX_2^+	DyX^+	Dy^+	Ref.
DyF_3	34	1430	0.50	100	20	19	this work
$DyCl_3$	50	1000	13.7	100	10.9	19.9	[7]
$DyCl_3$	25	1008	12.4	100	16.7	5.9	[8]
$DyBr_3$	15	1053	24.8	100	13.6	–	[9]
DyI_3	15	1053	69.9	100	–	–	[10]

Figure 1 shows the ionization efficiency curves (IEC) obtained for the different ions detected in DyF_3 vapors. Table 2 summarizes the appearance potentials obtained from the IEC curves for the ionic species of mass spectra recorded for different DyX_3 compounds. As expected, the ionization potentials of gaseous DyX_3 and the respective appearance potentials of the fragment ions increase on going from dysprosium iodide to dysprosium fluoride. However, the respective values for $DyCl_3$ and $DyBr_3$ are very similar in every case. The ionization and appearance potentials obtained experimentally should only be considered as an upper limit to the adiabatic values.[16]

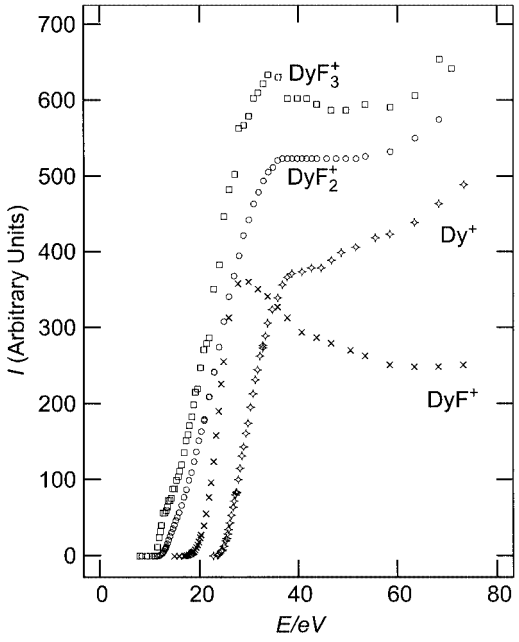

Figure 1. Ionization efficiency curves obtained for ions coming from DyF_3(g)

Theoretical Studies

The computed geometries, vibrational frequencies, and charge and spin densities on the Dy atom obtained for the neutral and ionized DyX (Table 3), DyX_2 (Table 4), and DyX_3 (Table 5) species are shown below. The bond length in DyX decreases significantly after the electron is removed (Table 3). The increased bond strength is indicated by a

Table 2. Experimental and theoretical ionization potentials and appearance potentials (in eV) of ions detected in the mass spectra of the DyX_3 vapors

DyX_3	Ref.(exp.)	IP (DyX_3) exp.	IP (DyX_3) theor.	AP (DyX_2^+) exp.	AP (DyX_2^+) theor.	AP (DyX^+) exp.	AP (DyX^+) theor.	AP (Dy^+) exp.	AP (Dy^+) theor.
DyF_3	this work	11.1	12.68	12.5	13.05	19.3	16.62	24.9	22.36
$DyCl_3$	[8]	10.0	10.42	11.4	11.87	15.1	14.49	20.1	18.06
$DyBr_3$	[9]	10.4	9.68	11.2	11.22	14.8	14.52	20.1	16.31
DyI_3	[24]	9.6	8.87	10.4	10.41	12.9	11.96	16.0	14.32

blue-shift of the stretching vibrations in the cations relative to the parent molecules. Spin-density calculations for DyX indicate four f and one s unpaired electrons on Dy. The ionization removes the nonbonding s electron and leads to an increase in the Coulomb interactions in the cation. Only the single valence electron from the s shell is involved in the Dy−X bond; the ionization removes the second one (Table 6). The charge transfer of 0.703 electrons from Dy to the halogen atom is not affected by the ionization process, indicating that the bond strength is enhanced mostly due to the increase in the ionic contribution.

The bonding in DyX_2 moieties is similar to that observed in DyX; the bond lengths are again shorter in the cations. The increasing strength of the bonds is confirmed by the blue-shifted stretching vibrational modes (Table 4). The polarization of the electronic density of the chemical bonds is similar to that in DyX. The charge transfer in the DyX_2 molecule is approximately double that in DyX. The spin-density analysis in the molecule as well as in the cation indicates the almost exclusive localization of the open-shell electrons on Dy. The ionization removes an electron from the f orbital; however, the loss of electronic density at the metal is compensated by the σ-back-donation of electrons from the halogens to the d and p valence-orbitals of dysprosium. The total atomic charge on the Dy center in $DyCl_2^+$ amounts to only 1.939 electrons (Table 6). The value of the positive charge localized on the central atom is consistent with the first two ionization potentials of Dy (5.927 eV and 11.67 eV).[17] The direct ionization of the f electron would involve about 20 eV (the third ionization potential of Dy is 22.8 eV [17]). A rearrangement of the electronic density on Dy is observed instead, and the loss of valence electrons from the f orbital of Dy is accompanied by σ-back-donation from the halogens.

The DyX_3 molecules follow trends observed in smaller compounds. The structures with C_{3v} symmetry are almost planar (Table 5). The experimental bond lengths are well reproduced by the present calculations.[18−20] The available vibrational frequencies for $DyCl_3$ (58, 85, 328, 340 cm^{-1} [18]) are in excellent agreement with the calculated values (56, 82, 331, 344 cm^{-1}). The Mulliken spin densities indicate the localization of unpaired electrons exclusively on the Dy atom, and the electron transfer from Dy to the halogen atoms is only slightly lower than the values of charge transfers in the DyX and DyX_2 molecules. However, the orbital electronic distribution on Dy is similar to that on the DyX_2^+ cation but not to its neutral precursors DyX and

Table 3. Theoretical bond lengths (r_e), stretching frequencies ($\tilde{\nu}_1$), total atomic charges (q) and atomic spin densities on dysprosium atoms in neutral and ionized DyX species

DyX	Electronic state molecule	Electronic state cation	r_e (Å) molecule	r_e (Å) cation	q(Dy) (electrons) molecule	q(Dy) (electrons) cation	Spin density (Dy) molecule	Spin density (Dy) cation	$\tilde{\nu}_1$ (cm^{-1}) molecule	$\tilde{\nu}_1$ (cm^{-1}) cation
DyF	6	5	2.020	1.971	0.632	1.707	5.110	4.009	497.9	581.1
DyCl	6	5	2.565	2.437	0.702	1.683	5.094	4.006	272.7	338.9
DyBr	6	5	2.711	2.586	0.724	1.653	5.041	4.004	180.9	236.2
DyI	6	5	2.969	2.809	0.702	1.579	5.024	4.013	139.5	179.8

Table 4. Theoretical bond lengths (r_e), bond angle (X−Dy−X), vibrational frequencies ($\tilde{\nu}$), total atomic charges (q) and atomic spin densities on the dysprosium atom in neutral and positively charged DyX_2 moieties

DyX_2	Electronic state molecule	Electronic state cation	r_e (Å) molecule	r_e (Å) cation	X−Dy−X (°) molecule	X−Dy−X (°) cation	q(Dy) (electrons) molecule	q(Dy) (electrons) cation	Spin density (Dy) molecule	Spin density (Dy) cation	$\tilde{\nu}$ (cm^{-1}) molecule	$\tilde{\nu}$ (cm^{-1}) cation
DyF_2	5	6	2.047	1.916	123.9	113.3	1.437	2.108	3.922	4.935	487.2	668.1 (ν_1)
											147.4	71.1 (ν_2)
											504.1	626.7 (ν_3)
$DyCl_2$	5	6	2.549	2.360	131.3	123.3	1.525	1.938	4.006	4.897	274.3	386.3 (ν_1)
											69.7	55.3 (ν_2)
											287.8	392.1 (ν_3)
$DyBr_2$	5	6	2.711	2.506	138.1	116.3	1.495	1.901	4.011	4.914	174.9	250.7 (ν_1)
											35.5	40.6 (ν_2)
											206.9	294.4 (ν_3)
DyI_2	5	6	2.938	2.799	143.6	140.7	1.417	1.742	4.019	4.652	127.4	122.3 (ν_1)
											27.3	28.4 (ν_2)
											169.3	350.6 (ν_3)

Table 5. Theoretical (r_e) and experimental (r_g) bond lengths, bond angle (X−Dy−X), total atomic charges (q) and atomic spin densities on the dysprosium atom in neutral and ionized DyX_3 species

DyX_3	Electronic state molecule	cation	R (Å) molecule[a]	cation[b]	X−Dy−X (°) molecule	cation[c]	q(Dy) (electrons) molecule	cation	Spin density (Dy) molecule	cation
DyF_3	6	5	2.012 2.09[d] 2.02[e]	1.918 (2.118)	119.9	121.2 (56.2)	2.000	2.057	4.973	3.045
$DyCl_3$	6	5	2.447 2.49[d] 2.47[e] 2.461[f]	2.335 (2.518)	118.9	113.3 (66.0)	1.810	1.785	4.983	4.982
$DyBr_3$	6	5	2.604 2.615[e] 2.609[f]	2.517 (2.673)	120.0	118.3 (69.2)	1.799	1.741	4.972	4.969
DyI_3	6	5	2.820 2.818[e]	2.758 (2.893)	120.0	122.5 (72.5)	1.644	1.600	4.941	4.886

[a] C_3v symmetry. [b] Cs symmetry. The distorted pyramid with halogen atoms at the base and one shorter and two longer (given in parentheses) bonds. [c] X_1-Dy-X_2 and X_2-Dy-X_2 (in parentheses) angles. [d] Ref.[18] [e] Ref.[19] [f] Ref.[20]

Table 6. The valence orbital populations on dysprosium from Mulliken and natural bond orbital (in parentheses) population analysis in $DyCl_n$ molecules and $DyCl_n^+$ cations ($n = 0-3$)

	s	p	d	f	Total charge on Dy atom
Dy	2.000 (0.000)	0.000 (0.000)	0.000 (0.000)	10.000 (10.000)	0.000 (0.000)
Dy^+	1.000 (1.000)	0.000 (0.000)	0.000 (0.000)	10.000 (10.000)	1.000 (1.000)
DyCl	1.108 (0.99)	0.040 (0.02)	0.140 (0.08)	10.009 (10.00)	0.703 (0.909)
$DyCl^+$	0.067 (0.05)	0.020 (0.01)	0.196 (0.13)	10.013 (10.00)	1.704 (1.816)
$DyCl_2$	0.160 (0.12)	0.090 (0.01)	0.240 (0.14)	9.984 (9.96)	1.525 (1.762)
$DyCl_2^+$	0.116 (0.07)	0.133 (0.01)	0.617 (0.411)	9.195 (9.15)	1.939 (2.360)
$DyCl_3$	0.197 (0.13)	0.230 (0.02)	0.623 (0.39)	9.139 (9.09)	1.811 (2.373)
$DyCl_3^+$	0.166 (0.09)	0.170 (0.01)	0.493 (0.31)	9.384 (9.34)	1.786 (2.240)

DyX_2. Two s and one f electrons of Dy are involved in the bond formation. The strong σ-back-donation to the d and p orbitals leads to a total charge of 1.811 electrons on Dy. Contrary to smaller systems the ionization of DyX_3 leads to dramatic changes. The unpaired electrons are no longer localized exclusively on the Dy center. The symmetry of the parent molecule (C_{3v}) is destroyed, and the cation undergoes a Jahn−Teller distortion, leading to C_s symmetry. The atomic charge localized on dysprosium is almost unchanged relative to the molecule, indicating a contribution of electronic density from the halogen atoms to the ionization process (Table 6). The consecutive ionization energies of dysprosium are 5.927, 11.67, and 22.8 eV. The active participation of halogen atoms in the ionization in the DyX_3 molecule is consistent with the increasing consecutive ionization potential of Dy. The third ionization potential (22.8 eV) is significantly higher than those (17.48, 13.01, 11.84, and 10.454 eV for F, Cl, Br, and I, respectively[21]) of the halogens.

For the reasons given in the previous section it was interesting to compare the experimental values of the ionization/fragmentation potentials with those obtained theoretically for adiabatic processes. The calculated ionization and appearance potentials are given in Table 2. The values generally agree with the respective potentials derived from the IEC taking into account the accuracy of experimental values of about ±0.5 eV. In most cases the theoretical values are somewhat smaller than the experimental ones. These differences become clearly larger for DyX^+ and Dy^+ ions in comparison to DyX_3^+ and DyX_2^+, probably due to the larger kinetic energy of two or three X fragments resulting in the fragmentation processes leading to these ions. More importantly, this agreement indicates the correct prediction of the structures of the studied species and validates the discussion concerning the nature of the bonding. In Figure 2 we display the ionization energies and energies of subsequent dissociations of the Dy−X bonds in the charged species obtained from the theoretical AP values in Table 2. The comparatively low dissociation energy of the first bond in the DyX_3^+ species could explain the highest intensity of the DyX_2^+ ions in all the mass spectra of dysprosium halides. The dissociation of subsequent halogen atoms from the ionic fragments becomes energetically less preferable. The tendency of increasing the dissociation energy of the Dy−X bond in going from the DyX_3^+ to the DyX^+ ionic species can be seen for all dysprosium halides with the exception of dysprosium bromide. At present we are not able to offer an explanation for this phenomenon.

Discussion and Conclusions

The mass spectrum patterns of the gaseous DyX_3 species consist of molecular ions and the DyX_2^+, DyX^+, and Dy^+ fragment ions, with DyX_2^+ being the most intense for all dysprosium halides. The ionization and appearance potentials obtained for these ions by quantum chemical methods

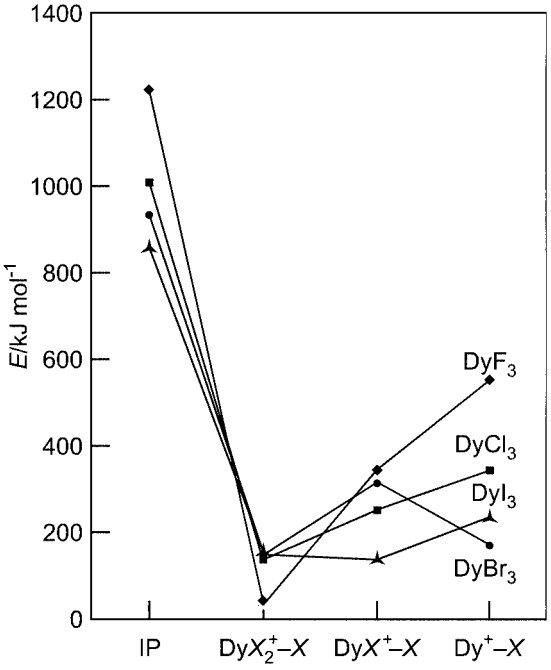

Figure 2. Ionization energies of DyX_3 and fragmentation energies for the DyX_n^+ ions ($n = 1-3$)

in the present study agree well with the experimental values. The thermodynamic meaning of the appearance potentials is the energy of dissociation of the metal−halide bonds in the neutral molecule. For instance, AP(DyF^+) correlates with the energy of the process

$$DyF_3(g) + e \rightarrow DyF^+ + 2F + 2e$$

Combinations of appearance potentials should yield the dissociation energies of the halogen−metal bond in ions. For instance the difference AP(DyF^+) − AP(DyF_2^+) should correlate with the energy of the dissociation process

$$DyF_2^+ \rightarrow DyF^+ + F$$

As already mentioned, the experimental appearance-potentials yield, in fact, upper limits of adiabatic values. Moreover, the accuracy of the AP values, usually reported, is no better than ±0.5 eV. Therefore the determination of the energies of the dissociation/fragmentation processes from experimental appearance potentials is limited.

The available experimental energetic data (ionization and appearance potentials) are reasonably reproduced by the calculated values. More importantly, the calculations reproduce the perturbations in the measured data that originate from the increasing importance of relativistic contributions in heavier halogens. The chemical bonds are formed due to the charge transfer of the electronic density from dysprosium to the halogen atoms. The atomic charge on Dy amounts to 0.702 (DyCl), 1.525 ($DyCl_2$), and 1.811 ($DyCl_3$) leading to a negative charge on chlorine of −0.702, −0.762, and −0.604 electrons, respectively. In the first-order approximation this electron transfer can be considered as an additive process. The increasing positive charge on the metal atom enhances the Coulomb interactions in the cations, leading to a shortening of the Dy−X distance. This charge transfer involves s electrons in DyX and DyX_2. In DyX_3, the f electrons also take part in the bonding (Table 6). The transfer of the f electron is compensated, however, by a similar amount of electronic density due to the σ-back-donation from halogen atoms to the d and p orbitals of Dy. The highest atomic charge in DyX_3 is close to two. This observation is consistent with the Dy values of the two lowest ionization potentials, which are smaller than those of the halogens. The open-shell electrons are localized almost exclusively on the dysprosium atom. The number of electrons confirms the involvement of one s, two s, and two s + one f electrons in the DyX, DyX_2, and DyX_3 bonding, respectively. The atomic charge on the metal atom in DyX_3 disagrees with the established model of the $Dy^{3+}X_3^-$ bonding scheme.[22] It is consistent, however, with the very high value of the third ionization potential of Dy. Due to the σ-back-donation of electrons from the halogens, a more appropriate model for the metallic center in DyX_3 is the Dy^{2+} cation in the excited electronic state, corresponding to an electron excitation from the f to the d orbital. The computations indicate the active participation of the f orbital in the bonding process in DyX_2^+ cations and DyX_3 molecules.

The ionization of DyCl removes the s electron, increasing the charge of Dy from 0.703 to 1.703 electrons. The ionization of $DyCl_2$ corresponds to the removal of the f electron. The charge on Dy increases from 1.525 to 1.939 electrons due to the compensation for electrons involved in the bonding by the σ-back-donation. The unpaired electrons are localized at the Dy center. The removal of the nonbonding f electron from the metal atom increases the Coulomb interactions. However, the ionization process does not affect the charge transfer. The increased contribution of the ionic interactions leads to shorter bonds. The effect of the increased bond strength is confirmed by a blue shift of the corresponding stretching vibrations. The ionization of DyX_3 is more complicated. Ionized $DyCl_3^+$ is subject to the Jahn−Teller effect, and the symmetrical C_{3v} molecules are distorted to the C_s geometry. The total spin-density indicates that open-shell electrons are also localized on the halogen atoms. The above observation agrees with the high values of the third IP of Dy and the preferred ionization of halogen atoms. Such a distribution of electronic density allows the value of the charge on the metallic center to be close to two electrons. The removal of the f electron is again compensated by the σ-back-donation. The bond formation and ionization processes in DyX, DyX^+, DyX_2, DyX_2^+, and DyX_3 lead to the electron loss from the Dy center involving less than two electrons. The primary process of the electron transfer from the metal (including the ionization process) is promptly compensated by the σ-back-donation from halogen atoms. The above processes are consistent with the two lowest IPs of Dy being lower than the first potentials of the halogens. An attempt to remove more electrons from Dy was not successful, and in the DyX_3^+ cation

the halogen atoms also contribute to the electron-loss process.

Experimental Section

Mass Spectra of Gaseous DyX_3: The mass spectrum of DyF_3 vapors and the ionization efficiency curves for ions identified in the mass spectrum were recorded on a CH5 mass spectrometer (Finnigan MAT, Bremen, Germany)[23] in Julich. Knudsen cells made of Mo with an edged effusion orifice of 0.8 mm diameter were employed in every case. The energy of the ionising electrons, 34 eV, was calibrated with the ionization potentials of Hg, In, and Ag measured prior to the recording of the DyF_3 mass spectra. Mass spectra and appearance potentials for ions present in the mass spectra of $DyCl_3$,[7,8] $DyBr_3$,[9] and DyI_3 [10] were taken from our previous studies. The mass spectrum of $DyCl_3$ [8] and the appearance potentials for ions in the DyI_3 mass spectrum[24] were also taken from the literature.

Theoretical Methods: The quantum-chemical calculations were carried out using the density functional theory (DFT) approach, using Becke's three-parameter functional[25] with Vosko et al.'s local correlation part[26] and Lee et al.'s[27] non-local part (abbreviated as B3LYP). All the calculations were carried out using the relativistic effective core potentials (RECPs) developed by the Stuttgart/Dresden groups that retain the outer $4s^24p^64d^{10}5s^25p^64f^{10}6s^2$ shells of dysprosium and ns^2np^7 of halogen atoms.[28–30] The corresponding basis sets are characterized as the (12s, 11p, 9d,8f) collection contracted to [5s, 5p, 4d, 2f] for Dy and (4s, 4p) contracted to [2s, 3p] for halogen atoms. The basis sets of the halogens were additionally supplemented by two d polarization and a set of sp diffuse functions proposed as part of the SDB-aug-cc-PVTZ and aug-cc-PVTZ basis sets.[31,32] Because of the ionic nature of the chemical bonds in the studied complexes, the validity of the basis sets was checked by the computation of the ionization potential of Dy and electron affinities of halogen atoms. The agreement between the calculated ionization potential of Dy (6.02 eV) and its experimental value (5.927 eV [17]) indicates the reasonable treatment of high-spin electronic states in the Dy atom (sextet) as well as in the Dy^+ cation (quintet) within the applied density functional theory method. The theoretical values of electronic affinities for F (3.33 eV), Cl (3.72 eV), Br (3.51 eV), and I (3.35 eV) agree satisfactorily with the respective experimental data of 3.401, 3.61, 3.36, and 3.059 eV.[21] The availability of unpaired electrons on the f orbitals of dysprosium allows for the rich manifold of electronic states in the studied compounds. The calculations for the studied molecules and cations were performed for the different electronic states allowed by the electronic configurations of the participating atoms, to ensure the location of the proper electronic ground state. Spin-orbit contributions have been neglected in the present calculations. Previous calculations, which estimated such contributions for lanthanide trihalides,[33] indicated that although not negligible, spin-orbit effects constitute only a few percent of the studied properties and do not change the qualitative picture. All geometrical structures were optimized. The location of true minima was confirmed in calculations of vibrational frequencies. The electronic density distributions were studied applying the Mulliken population analysis and the natural bond orbital (NBO) analysis.[34] Because both approaches lead to a similar qualitative picture, the results of the Mulliken populations are discussed in detail in the text. Although differences in electronegativity between halogen atoms lead to some quantitative differences,[34] the qualitative picture of the electron-density distribution is similar and detailed results are illustrated for dysprosium chloride. The calculations were carried out using the Gaussian 98 package of programs.[35]

Acknowledgments

This work was facilitated in part by the Polish State Committee for Scientific Research under grant 3 T09A 020 19, NSF Grant No. 9805465 & 9706268, ONR Grant No. N00014−98-1-0592, and the Army High Performance Computing Research Center under the auspices of the Department of the Army, Army Research Laboratory cooperative agreement number DAAH04−95-2-0003/contract number DAAH04−95-C-0008. This work does not necessarily reflect the policy of the government, and no official endorsement should be inferred. We would like to thank the Mississippi Center for Supercomputing Research, Poznan and Wroclaw Supercomputing and Networking Centers, and the Interdisciplinary Center for Mathematical and Computational Modeling of Warsaw University for a generous allotment of computer time.

[1] D. Schroeder, J. Loos, H. Schwarz, R. Thissen, O. Dutuit, *Inorg. Chem.* **2001**, *40*, 3161.
[2] R. G. Cooks, P. S. H. Wong, *Acc. Chem. Res.* **1998**, *31*, 379.
[3] G. Wang, R. B. Cole, *J. Electr. Spectr. Rel. Phenomen.* **2000**, *108*, 153.
[4] L. N. Gorokhov, *Proc. II Int. Symp. on High Temperature Mass Spectrometry*, July 7−10, 2003, Plyos, Russia, p. 57.
[5] J. C. Lorquet, *Int. J. Mass Spectrom.* **2000**, *200*, 43.
[6] B. Brunetti, P. Vassallo, V. Piacente, P. Scardala, *J. Chem. Eng. Data* **1999**, *44*, 509.
[7] J. Kapała, S. Roszak, S. Nunziante Cesaro, M. Miller, *J. Alloys Comp.* **2002**, *345*, 90.
[8] Yu. Kuznetsov, M. F. Butman, L. S. Kudin, A. M. Pogrebnoi, G. G. Burdukovskaja, *Teplofiz. Vys. Temp.* **1997**, *35*, 731; *Chem. Abstr.* **1998**, *128*, 7741n.
[9] K. Hilpert, M. Miller, F. Ramondo, *J. Chem. Phys.* **1995**, *102*, 6194.
[10] K. Hilpert, M. Miller, F. Ramondo, *Thermochim. Acta*, in press.
[11] L. Joubert, G. Picard, J.-J. Legendre, *Inorg. Chem.* **1998**, *37*, 1984.
[12] A. Kovacs, R. J. M. Konings, *Vibr. Spectr.* **1997**, *15*, 131.
[13] V. G. Solomonik, O. Y. Marochko, *J. Struct. Chem.* **2000**, *41*, 725.
[14] A. Kovacs, *J. Mol. Struct.* **1999**, *482/483*, 403.
[15] J. W. Hastie, in *High Temperature Vapors, Materials Science and Technology Series*, Academic Press, New York, **1975**, p. 91.
[16] J. A. Morris, in *Mass spectrometry, Vol. 5, MTP International Review of Science, Physical Chemistry Series 1* (Ed.: A. Maccoll), Butterworths, London, **1972**.
[17] W. C. Martin, L. Hagan, J. Reader, J. Sugar, *J. Phys. Chem. Ref. Data* **1974**, *3*, 771.
[18] E. Myers, D. T. Graves, *J. Chem. Eng. Data* **1977**, *22*, 436.
[19] M. Hargittai, *Coord. Chem. Rev.* **1988**, *91*, 35.
[20] M. Hargittai, *Chem. Rev.* **2000**, *100*, 2233.
[21] *CRC Handbook of Chemistry and Physics, 83rd Edition* (Ed.: D. R. Lide), CRC Press, Boca Raton, **2002**.
[22] *Lanthanide and Actinide Chemistry and Spectroscopy, ACS Symp. Series 131* (Ed.: N. M. Edelstein), ACS, Washington D. C., **1980**.
[23] K. Hilpert, *J. Electrochem. Soc.* **1989**, *136*, 2099.
[24] O. Kaposi, L. Lelik, A. Balthazar, *High Temp. Sci.* **1983**, *16*, 299.
[25] D. Becke, *J. Chem. Phys.* **1993**, *98*, 5648.
[26] S. H. Vosko, L. Wilk, M. Nusiar, *Can. J. Phys.* **1980**, *58*, 1200.
[27] C. Lee, W. Yang, R. G. Parr, *Phys. Rev. B* **1988**, *37*, 785.
[28] M. Dolg, H. Stoll, H. Preuss, R. M. Pitzer, *J. Phys. Chem.* **1993**, *97*, 5852.

[29] A. Bergner, M. Dolg, W. Kuechle, H. Stoll, H. Preuss, *Mol. Phys.* **1993**, *80*, 1431.
[30] W. Kuechle, M. Dolg, H. Stoll, H. Preuss, *Mol. Phys.* **1991**, *74*, 1245.
[31] E. Woon, T. H. Dunning Jr., *J. Chem. Phys.* **1995**, *103*, 4572.
[32] J. M. L. Martin, A. Sundermann, *J. Chem. Phys.* **2001**, *114*, 3408.
[33] E. Reed, L. A. Curtiss, F. Weinhold, *Chem. Rev.* **1988**, *88*, 899.
[34] C. Adamo, P. Maldivi, *J. Phys. Chem. A* **1998**, *102*, 6812.
[35] M. J. Frisch, G. W. Trucks, H. B. Schlegel, G. E. Scuseria, M. A. Robb, J. R. Cheeseman, V. G. Zakrzewski, J. A. Montgomery, Jr., R. E. Stratmann, J. C. Burant, S. Dapprich, J. M. Millam, A. D. Daniels, K. N. Kudin, M. C. Strain, O. Farkas, J. Tomasi, V. Barone, M. Cossi, R. Cammi, B. Mennucci, C. Pomelli, C. Adamo, S. Clifford, J. Ochterski, G. A. Petersson, P. Y. Ayala, Q. Cui, K. Morokuma, N. Rega, P. Salvador, J. J. Dannenberg, D. K. Malick, A. D. Rabuck, K. Raghavachari, J. B. Foresman, J. Cioslowski, J. V. Ortiz, A. G. Baboul, B. B. Stofanov, C. Liu, A. Liashenko, P. Piskorz, I. Komaromi, R. Gomperts, R. L. Martin, D. J. Fox, T. Keith, M. A. Al-Laham, C. Y. Peng, A. Nanayakkara, M. Challacombe, P. M. W. Gill, B. Johnson, W. Chen, M. W. Wong, J. L. Andres, C. Gonzalez, M. Head-Gordon, E. S. Replogle, J. A. Pople, *Gaussian 98, Revision A.11.3*, Gaussian, Inc., Pittsburgh PA, **2002**.

Received September 3, 2003
Early View Article
Published Online February 10, 2004

